Chemical Engineering Journal 152 (2009) 396–405

Contents lists available at ScienceDirect

Chemical Engineering Journal

journal homepage: www.elsevier.com/locate/cej

Simulation of CO_2 absorption into aqueous DEA using a hollow fiber membrane contactor: Evaluation of contactor performance

José A. Delgado*, María A. Uguina, José L. Sotelo, Vicente I. Águeda, Abel Sanz

Department of Chemical Engineering, Universidad Complutense de Madrid, Av. Complutense s/n, 28040 Madrid, Spain

ARTICLE INFO

Article history:
Received 6 February 2009
Received in revised form 22 April 2009
Accepted 28 April 2009

Keywords:
Hollow fiber membrane module
Diethanolamine
Carbon dioxide
Contactor performance
Lean carbon dioxide loading
Productivity

ABSTRACT

The absorption of carbon dioxide from a carbon dioxide/nitrogen mixture into an aqueous diethanolamine solution (as an example of a typical amine solution) using a hollow fiber contactor is simulated to obtain the effect of several operational variables (liquid velocity, fiber length, lean carbon dioxide loading, and amine concentration) on productivity and amine solution to carbon dioxide ratio. The model employed is based on the ones commonly used in the literature for this process, but it was significantly improved as some simplifications usually considered (irreversible reaction, low carbon dioxide loading, constant partition coefficient of molecular carbon dioxide between liquid and gas phases, absence of bicarbonate and carbonate anions) have been removed. The effect of these simplifications on the simulated results is quite important. A simple performance parameter study is proposed to evaluate the contactor's performance, keeping the feed gas concentration and the fraction of carbon dioxide removal constant. This procedure leads to optimum values of the liquid velocity and lean carbon dioxide loading, while the performance parameter improves with amine concentration.

1. Introduction

The emission of carbon dioxide into the atmosphere due to the consumption of large amounts of fossil fuels has become one of the most serious environmental problems, which is now being paid attention to by public authorities worldwide. Fuel powered power plants are an important source of these emissions. A possible way for reducing the carbon dioxide emissions can be to include a removal system in these installations [1]. Thus, the development of carbon dioxide capture systems has attracted much attention nowadays, which must fit the required carbon dioxide separation performance with a minimal energy penalty [2]. The most widely established method for this purpose is to remove carbon dioxide by absorption into aqueous alkanolamine solutions in conventional contactor equipment [3]. The use of microporous membranes to carry out the absorption process offers significant advantages with respect to conventional absorption columns [4,5]. Because of these advantages, extensive research has been carried out on carbon dioxide capture by chemical absorption using hollow fiber membrane contactors [4–9]. In these processes, it is highly desirable that the hydrophobicity of the membrane is high enough to avoid membrane wetting (i.e., filling of membrane micropores with the liquid solution), so as to minimize the mass transfer resistance in the membrane. The influence of membrane wetting on carbon dioxide capture by aqueous DEA with polypropylene microporous hollow fiber membranes has been studied by many authors [10–15]. Although the carbon dioxide flux decreases significantly due to this phenomenon, the initial flux can be restored by drying the membrane or increasing slightly the gas pressure (about a 10% over the atmospheric pressure [14]).

All these works have helped to get a good insight about the functioning of hollow fiber membrane contactors for carbon dioxide capture with aqueous amines. However, it must be noted that they have mainly been focused on understanding the effect of operational variables on the removal behaviour of carbon dioxide, evaluated with the fraction of carbon dioxide removal, the average flux of carbon dioxide, and the overall mass transfer coefficient. Less attention has been devoted to the cost of the regeneration of the amine loaded with carbon dioxide. In order to minimize the circulating flow rate of amine (and accompanying water) in the process and the energy of regeneration, the ratio of amine solution to dissolved carbon dioxide must be minimum [16]. Another important parameter affecting the regeneration energy is the remaining carbon dioxide to amine ratio after regeneration (lean carbon dioxide loading). The regeneration energy per unit mass of carbon dioxide relates inversely to the lean carbon dioxide loading [17].

In most of the studies commented before, an irreversible reaction is usually considered, neglecting the reverse reaction step. This assumption is not valid for the carbon dioxide/amine ratios typically found in real systems (0.10.5 mol_{CO_2}/mol_{amine} [17]). Recently,

* Corresponding author. Tel.: +34 91 3944119; fax: +34 91 3944114.
E-mail address: jadeldob@quim.ucm.es (J.A. Delgado).

1385-8947/$ – see front matter © 2009 Elsevier B.V. All rights reserved.
doi:10.1016/j.cej.2009.04.064

Boucif et al. [18] have taken into account the reversibility of the reaction between carbon dioxide and amine in a hollow fiber contactor. However, several simplifications are assumed by these authors: (i) the lean carbon dioxide loading is zero, (ii) the presence of bicarbonate and carbonate is neglected and (iii) the variation of the partition coefficient (dissolved molecular carbon dioxide concentration/carbon dioxide concentration in gas) with carbon dioxide and amine concentrations is not considered. As it is discussed later, the effects of these parameters may be quite important.

In this work, the absorption of carbon dioxide from a carbon dioxide/nitrogen mixture into an aqueous DEA solution (as an example of a typical amine solution) using a hollow fiber contactor is simulated to obtain the effect of several operational variables (liquid velocity, fiber length, lean carbon dioxide loading, and amine concentration) on productivity and amine solution to carbon dioxide ratio. The model employed is based on the ones commonly used in the literature for this process, but it was significantly improved as the simplifications in previous studies have been removed. The effect of these simplifications on the simulated results is studied.

2. Model description

The model is divided into two submodels: the transport model for the hollow fiber contactor, and the kinetic model for describing the reaction between CO_2 and DEA in water. The most important contributions of this work are the improvement of the kinetic model for the reaction between CO_2 and alkanolamines in water and the way of assessing the system performance. It must be noted that the model employed has not been validated with experimental results. The transport model is based on assumptions (described below) widely accepted for this kind of systems [5,7–9,19], which have been validated experimentally, so it is reasonable to expect that the proposed equations are also valid with the kinetic model proposed. An experimental validation of the kinetic model is required to check its reliability in a rigorous manner. However, as it is based on fundamental equations, where the kinetic parameters have been obtained from experimental studies in the literature, and the equilibrium parameters have been obtained from AspenPlus®, which is a reliable simulation package for simulating the chemical absorption of carbon dioxide into aqueous DEA [20], one may also expect that the model predictions are reliable. The validation of the kinetic model will be the subject of future works.

2.1. Kinetic model for the reaction between CO_2 and DEA in water

The kinetic model for describing reaction kinetics between carbon dioxide and DEA in water has been developed according to the zwitterion mechanism [21,22], which is widely accepted for the reaction between carbon dioxide and primary or secondary amines. This mechanism comprises the following steps for DEA:

$$CO_2 + DEA \underset{k_z^{-1}}{\overset{k_z}{\rightleftarrows}} \text{Zwitterion} \quad (1)$$

$$\text{Zwitterion} + DEA \underset{k_D^{-1}}{\overset{k_D}{\rightleftarrows}} DEACOO^- + DEA^+ \quad (2)$$

$$\text{Zwitterion} + H_2O \underset{k_H^{-1}}{\overset{k_H}{\rightleftarrows}} DEADOO^- + H_3O^+ \quad (3)$$

where $DEACOO^-$ is the amine carbamate ion and DEA^+ is the protonated amine. The zwitterion is an intermediate species deprotonated by all the bases present in the reaction medium (DEA, H_2O and OH^- in an aqueous solution of DEA). According to Versteeg and Swaaij [23], the contribution of the hydroxyl ions to the deprotonation of the zwitterion may be neglected without a substantial loss of accuracy. Unfortunately, not all the kinetic parameters in this reaction scheme are available in the literature, but only some combinations of them. The values of k_z, $k_D k_z/k_z^{-1}$ and $k_H k_z/k_z^{-1}$ at several temperatures for the CO_2–DEA–H_2O system are given by Littel et al. [22]. With these parameter values, the forward reaction rate can be estimated (assuming the steady state approximation for the zwitterions [22]), whereas the reverse rates of reactions (2) and (3), and the distribution of products at equilibrium, require more parameters. This distribution may be calculated by employing an equilibrium speciation model such as the one provided by AspenPlus® (ELECNRTL), which considers the following equilibria for the CO_2–DEA–H_2O system:

$$DEA^+ + H_2O \overset{K_1}{\longleftrightarrow} DEA + H_3O^+ \quad (4)$$

$$DEACOO^- + H_2O \overset{K_2}{\longleftrightarrow} DEA + HCO_3^- \quad (5)$$

$$2H_2O \overset{K_3}{\longleftrightarrow} H_3O^+ + OH^- \quad (6)$$

$$CO_2 + 2H_2O \overset{K_4}{\longleftrightarrow} H_3O^+ + HCO_3^- \quad (7)$$

$$HCO_3^- + H_2O \overset{K_5}{\longleftrightarrow} H_3O^+ + CO_3^{2-} \quad (8)$$

where K_{1-5} are the corresponding equilibrium constants. By summing reactions (1) and (2), and (1) and (3), it is deduced that:

$$\frac{[DEACOO^-][DEA^+]}{[CO_2][DEA]^2} = \frac{k_z}{k_z^{-1}}\frac{k_D}{k_D^{-1}} \quad (9)$$

$$\frac{[DEACOO^-][H_3O^+]}{[CO_2][DEA][H_2O]} = \frac{k_z}{k_z^{-1}}\frac{k_H}{k_H^{-1}} \quad (10)$$

Thus, if the total amounts of CO_2, DEA and H_2O in both ionic and molecular forms are fixed, the values of k_D^{-1} and k_H^{-1} can be calculated from the resulting concentrations at equilibrium and the available combinations of parameters. The ELECNRTL model also allows the estimation of the diffusivities of all of the dissolved species and the partition coefficient (which includes the vapor phase fugacity):

$$H = \frac{[CO_2]}{[CO_2]_{gas}} \quad (11)$$

If k_D^{-1} and k_H^{-1} are known, the overall rate of reactions (1)–(3), including the reverse reaction rate, can be calculated by applying the steady state approximation for zwitterions ($d[Z]/dt = 0$):

$$r_1 = \frac{(k_D k_z/k_z^{-1})[CO_2][DEA]^2 + (k_H k_z/k_z^{-1})[CO_2][DEA][H_2O] - k_D^{-1}[DEACOO^-][DEA^+] - k_H^{-1}[DEACOO^-][H_3O^+]}{(1/k_z)(k_z + (k_D k_z/k_z^{-1})[DEA] + (k_H k_z/k_z^{-1})[H_2O])} \quad (12)$$

$$r_2 = \frac{(k_D k_z/k_z^{-1})[CO_2][DEA]^2 + (k_D k_H^{-1}/k_z^{-1})[DEACOO^-][H_3O^+][DEA] - k_D^{-1}[DEACOO^-][DEA^+] - (k_D^{-1} k_H/k_z^{-1})[DEACOO^-][DEA^+][H_2O]}{(1/k_z)(k_z + (k_D k_z/k_z^{-1})[DEA] + (k_H k_z/k_z^{-1})[H_2O])} \quad (13)$$

$$r_3 = \frac{(k_H k_z/k_z^{-1})[CO_2][DEA][H_2O] + (k_H k_D^{-1}/k_z^{-1})[DEACOO^-][DEA^+][H_2O] - k_H^{-1}[DEACOO^-][H_3O^+] - (k_D k_H^{-1}/k_z^{-1})[DEA][DEACOO^-][H_3O^+]}{(1/k_z)(k_z + (k_D k_z/k_z^{-1})[DEA] + (k_H k_z/k_z^{-1})[H_2O])} \quad (14)$$

It may be checked that reaction (4) can be obtained as reaction (3)–reaction (2), and reaction (5) as reaction (7)–(reaction (1) + reaction (3)). Therefore, reactions (4) and (5) can be replaced by reactions (1)–(3) in the reaction scheme provided by the ELECNRTL model without changing the distribution of products at equilibrium. The overall rates of reactions (6)–(8) were calculated with the following expressions:

$$r_6 = k_6[H_2O]^2 - \frac{k_6}{K_3}[H_3O^+][OH^-] \quad (15)$$

$$r_7 = k_7[CO_2][H_2O]^2 - \frac{k_7}{K_4}[H_3O^+][HCO_3^-] \quad (16)$$

$$r_8 = k_8[HCO_3^-][H_2O] - \frac{k_8}{K_5}[H_3O^+][CO_3^{2-}] \quad (18)$$

The values of k_6, k_7 and k_8 were fixed by increasing them progressively until the effect on the simulated results was negligible, so that the corresponding reactions are at equilibrium at any time. The reaction rate for any compound can be calculated from the overall rates of the reactions where the compound appears or disappears (for example, $-d[CO_2]/dt = r_1 + r_7$). With the proposed kinetic model, the reaction rate is calculated reasonably well taking into account the available kinetic parameters, since the rate controlling step in the formation of carbamates in the CO_2–DEA–H_2O system is the deprotonation of the zwitterion (reactions (2) and (3) [24]), and the distribution of products reaching equilibrium is correct, because it is the same as the one predicted by the ELECNRTL model.

It has been assumed that the reaction takes place at 40 °C, which lies within the typical range of temperature in a carbon dioxide absorption process from flue gases with amines [3,25]. The two amine concentrations analyzed (2 and 5 M) are within the typical range of conventional absorption systems [17,20]. The values of k_z, $k_D k_z/k_z^{-1}$ and $k_H k_z/k_z^{-1}$ taken from Littel et al. [22] are given in Table 1. It was assumed that these values do not change with carbon dioxide and amine concentration, as their dependence on these variables is not available. The rest of the parameters estimated from the results of the ELECNRTL model for the carbon dioxide and amine concentrations considered in this work are given in Table 2. For a given amine concentration, the dependence of k_D^{-1}, k_H^{-1}, K_3, K_4, K_5 and H on carbon dioxide concentration was described by polynomial interpolation. For simplicity, the liquid diffusivities were assumed to be constant for a given amine concentration (average value in Table 2), and the partition coefficient was assumed to be constant along the hollow fibers, equal to the average value between the inlet and the outlet.

Table 1
Kinetic parameters for the reaction between CO_2 and DEA at 40 °C [22].

DEA concentration range (mol m^{-3})	150–2500
k_z (m^3 mol^{-1} s^{-1})	6.19
$k_D k_z/k_z^{-1}$ (m^6 mol^{-2} s^{-1})	1.34×10^{-3}
$k_H k_z/k_z^{-1}$ (m^6 mol^{-2} s^{-1})	1.423×10^{-5}

2.2. Transport model for the hollow fiber contactor

A numerical model has been developed to describe the absorption of carbon dioxide on an aqueous DEA solution, based on the ones employed by Gong et al. [9] and Zhang et al. [5]. The carbon dioxide/nitrogen mixture and aqueous DEA solution are fed counter-currently to the shell and lumen side of the contactor, respectively. The model proposed in this work has a distinct feature with respect to the literature models: the mole flow rate of each component is considered as the dependent variable in the shell side, instead of the concentration of each component and the gas velocity. This approach allows solving the mass balance in the shell side without the need of an iterative calculation for each integration step [5], and avoiding the discretization in the radial direction of this zone [9]. The rest of assumptions are: (i) steady state and isothermal condition, (ii) plug flow in the axial direction both in the gas and liquid sides and (iii) fully developed parabolic liquid velocity profile inside the hollow fiber. The assumption of plug flow in the gas and liquid sides implies that axial diffusion is neglected. Radial diffusion in the shell side is modeled with a linear driving force approximation, using an engineering correlation, as it is discussed later. These assumptions, which have been validated experimentally by Yeon et al. [7] and Gong et al. [9], were considered because they simplify the model resolution notably. It must be noted that the effect of axial dispersion is important only for low values of the Peclet number (fluid velocity × fiber length/dispersion coefficient < 50) which are not considered in this work.

Fig. 1 shows a scheme of the hollow fiber contactor and the concentration profile considered. The differential mass balance for carbon dioxide in the shell side is

$$\frac{dF_A}{dz} = K_G 2\pi R_0 (C_A - C_{A,L}) \quad (19)$$

Table 2
Model parameters at 40 °C estimated from the results of the ELECNRTL model for the CO_2–DEA–H_2O system (AspenPlus®).

Total [DEA] (mol m^{-3})	Total [CO_2] (mol m^{-3})	D_{H_2O}[a]	D_{CO_2}	D_{DEA}	D_{DEA+}	D_{H_3O}	D_{DEACOO}	D_{HCO_3}	D_{OH}	D_{CO_3}	H	k_D^{-1}[b]	k_H^{-1}[c]	K_3[d]	K_4[e]	K_5[f]
2000	8	5.19	2.33	1.11	1.40	9.79	1.40	1.52	5.54	0.97	0.51	2.43	43.2	1.61	3.04	1.94
2000	200	5.41	2.42	1.15	1.38	9.70	1.38	1.51	5.49	0.96	0.47	1.04	17.4	3.21	6.85	6.90
2000	595	5.89	2.60	1.25	1.36	9.53	1.36	1.48	5.39	0.94	0.41	0.38	8.00	4.60	12.6	13.5
2000	966	6.28	2.76	1.34	1.34	9.37	1.34	1.46	5.31	0.93	0.36	0.23	5.64	4.85	16.0	16.1
2000	1528	6.36	2.86	1.40	1.30	9.14	1.30	1.42	5.18	0.90	0.34	0.21	5.26	4.56	17.5	16.2
5000	26	2.81	1.36	0.60	1.40	9.77	1.39	1.51	5.53	0.97	0.34	3.23	37.9	3.31	7.21	2.94
5000	256	3.01	1.44	0.64	1.37	9.63	1.37	1.50	5.45	0.95	0.31	1.47	14.1	6.46	17.1	11.3
5000	1252	4.05	1.88	0.86	1.29	9.04	1.29	1.41	5.12	0.89	0.19	0.30	4.75	5.56	31.8	18.4
5000	2494	5.79	2.57	1.23	1.19	8.30	1.19	1.29	4.70	0.82	0.12	0.22	5.87	1.69	19.0	8.17
5000	2720	5.99	2.65	1.28	1.16	8.16	1.16	1.27	4.62	0.81	0.12	0.24	6.98	1.41	16.6	7.13

[a] Diffusivities in the liquid phase (10^{-9} m^2 s^{-1}).
[b] Multiply by 10^{-3} m^3 mol^{-1} s^{-1}.
[c] Multiply by 10^4 m^3 mol^{-1} s^{-1}.
[d] Multiply by 10^{-17}.
[e] Multiply by 10^{-13} m^3 mol^{-1}.
[f] Multiply by 10^{-12}.

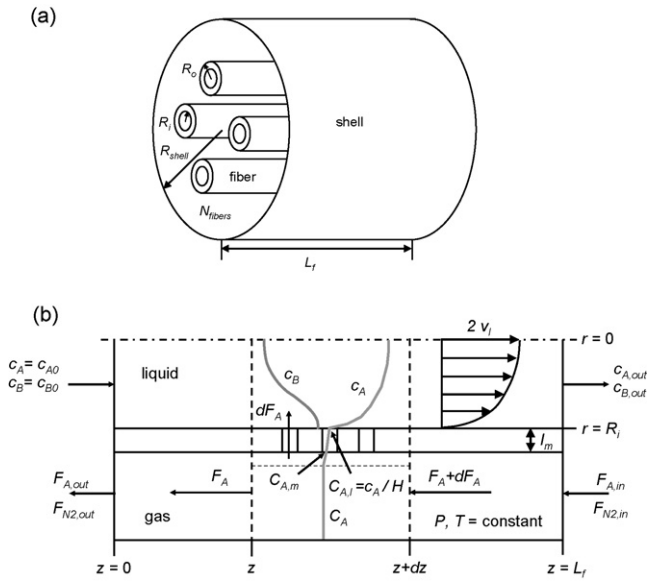

Fig. 1. Schematic diagrams of the hollow fiber contactor. (a) Geometry. (b) Gas and liquid flow, assumed concentration profile, and model parameters. F_A and F_{N_2} are the total mole flow rates of CO_2 and N_2 fed to the shell side of the contactor divided into the number of fibers, all the fibers being equivalent.

where F_A is the mole flow rate of carbon dioxide distributed among all the fibers (total carbon dioxide flow rate/N_{fibers}), K_G is the overall mass transfer coefficient between gas and liquid surface, C_A is the carbon dioxide concentration in the gas bulk, and $C_{A,L}$ is the carbon dioxide concentration in the gas in contact with the liquid phase. Local equilibrium is assumed between both phases, so that the relationship between the interphase concentrations is

$$C_{A,L} = \frac{c_A}{H} \tag{20}$$

where c_A is the concentration in the liquid interphase. For nitrogen, it is assumed that the flux of nitrogen diffusing into the membrane pores is negligible, due to its low solubility, so the mass balance is the continuity of mole flow rate ($F_{N_2} = F_{N_2,\text{in}} = F_{N_2,\text{out}}$). C_A is calculated from

$$C_A = \frac{P}{RT}\frac{F_A}{F_A + F_{N_2}} \tag{21}$$

The global mass transfer coefficient is given by

$$K_G = \left(\frac{1}{k_g} + \frac{l_m R_0}{D_{A,g} R_{lm}}\right)^{-1} \tag{22}$$

where k_g is the individual mass transfer coefficient in the shell side, $D_{A,g}$ is the effective diffusion coefficient of carbon dioxide in membrane pores, l_m is the membrane thickness, R_0 is the external fiber radius and R_{lm} is the log-mean radius of the fiber. $D_{A,g}$ was calculated with Bonsaquet equation assuming that the membrane pores are filled with gas, and that only diffusive flux takes place (taking into account molecular and Knudsen diffusivities), which is usually considered in this system for the non-wetted mode [8,9,26]. A slight overpressure in the shell side is assumed to get this condition (0.1 bar, Table 3 [14]). This situation was considered because it leads to the best contactor performance [9]. The mass transfer coefficient in the shell side (k_g) was calculated with the correlation proposed by Prasad and Sirkar [27], valid for shell side flow parallel to the fibers according to the geometry of the Celgard 1.7 × 5.5 MiniModule®:

$$Sh_g = 5.85(1-\phi)\left(\frac{d_h}{L_f}\right) Re_g^{0.6} Sc_g^{0.33} \tag{23}$$

Table 3
Model parameters used in the simulations.

R_i (m)	1.1×10^{-4}
R_0 (m)	1.5×10^{-4}
l_m (m)	4.0×10^{-4}
L_f (m)	0.113
R_{shell} (m)	0.021
ϕ	0.37
N_{fibers}	7400
P (Pa)	1.1×10^5
T (K)	313
$D_{A,g}$ ($m^2\ s^{-1}$)	4.64×10^{-7}
$D_{A,m}$ ($m^2\ s^{-1}$)	1.63×10^{-5}
ρ_g ($kg\ m^{-3}$)	1.29
μ_g (Pa s)	1.79×10^{-5}
$y_{A,in}$ (CO_2 mole fraction in feed gas)	0.13
θ	0.9

where Sh_g is the Sherwood number, ϕ is the packing fraction, Re_g is the Reynolds number and Sc_g is the Schmidt number. Constant gas density and viscosity estimated at feed conditions (ideal gas law and Wilke equation [28]), and the average value of gas velocity between inlet and exit, are employed in the calculation of k_g. The initial condition for Eq. (19) is

$$z = 0, \quad F_A = F_{A,\text{in}}(1-\theta) \tag{24}$$

where $F_{A,\text{in}}$ is the carbon dioxide mole flow rate at the inlet, and θ is the fraction of carbon dioxide removal. A value of $\theta = 0.9$ was used in all the simulations, that is, a 90% recovery of carbon dioxide from flue gas. The differential mass balance for any component in the liquid side is

$$v_z \frac{\partial c_i}{\partial z} = \frac{D_{i,L}}{r}\frac{\partial}{\partial r}\left(r\frac{\partial c_A}{\partial r}\right) - r_i \tag{25}$$

where v_z is the liquid velocity, $D_{i,L}$ is the liquid diffusivity of ith component, r is the radial coordinate, and r_i is the reaction rate of ith component ($r_i = -\text{d}[i\text{th component}]/\text{d}t$, calculated from the kinetic model). The dependence of v_z on r is given by

$$v_z = 2v_L(1-x^2) \quad x = \frac{r}{R_i} \tag{26}$$

where v_L is the average liquid velocity. The "mixed cup" average concentration [29] of any component is

$$\bar{c}(z) = \int_0^1 4(1-x^2)c(x,z)x\,\text{d}x \tag{27}$$

Therefore, the mole flow rate of ith component in the liquid side at each axial position is

$$F_{i,L} = v_L \bar{c}_i \pi R_i^2 \tag{28}$$

The initial concentration of each component at any radial position in the liquid amine (for a given lean carbon dioxide loading and total amine concentration) was calculated assuming that the mixture is at equilibrium, solving the system of equations including the mass balances of CO_2, DEA and H_2O, the charge balance, and the equilibrium equations corresponding to reactions (6)–(8) and Eqs. (9) and (10).

The boundary conditions for the radial coordinate are

$$\begin{aligned} r = 0, &\quad \frac{\partial c_A}{\partial r} = 0 \\ r = R_i, &\quad \frac{\partial c_A}{\partial r} = \frac{K_G R_0}{D_{A,L} R_i}(C_A - C_{A,L}) \\ r = 0, &\quad \frac{\partial c_B}{\partial r} = 0 \\ r = R_i, &\quad \frac{\partial c_B}{\partial r} = 0 \end{aligned} \tag{29}$$

Table 4
Parameter values of the Celgard 1.7 × 5.5 MiniModule®.

Parameter	Value
Number of fibers	7400
Fiber internal diameter (μm)	220
Fiber outer diameter (μm)	300
Effective pore size (μm)	0.03
Tortuosity	2.7
Diameter (m)	0.0425
Effective fiber length (m)	0.113

where B indicates any component in the liquid phase different from molecular CO_2. The values of the transport model parameters used in the simulations are given in Table 3. The contactor dimensions have been taken from the brochure of a commercial hollow fiber contactor (Celgard 1.7 × 5.5 MiniModule®, Table 4).

The complete model was solved numerically using the PDECOL package (FORTRAN version of 1987), a public domain code which uses orthogonal collocation on finite elements technique. This package is based on the method of lines and uses a finite element collocation procedure (with piecewise polynomials as the trial space) for the discretization of the dimensionless spatial variable x. The collocation procedure reduces the PDE system to a semi-discrete system which then depends on the variable with an initial condition only (z in this case). The initial concentrations in the liquid phase were calculated with the FCN subroutine of the IMSL library. As the carbon dioxide mole flow rate in the gas phase is not known a priori at $z = 0$, an external iteration is necessary to solve the model for a fixed carbon dioxide concentration in the gas phase at $z = L_f$ and a fixed fraction of carbon dioxide removal (θ). A simple substitution method with relaxation iterating with $F_{A,\text{in}}$ was used for this purpose.

3. Results and discussion

3.1. Effect of liquid velocity, reversibility of the deprotonation steps, formation of bicarbonate and carbonate, and variation of partition coefficient

Fig. 2 shows the effect of liquid velocity on contactor performance for the following conditions: total [DEA] = 2000 mol m^{-3}, total [H_2O] = 44,000 mol m^{-3}, lean carbon dioxide loading = 0.25. The maximum liquid velocity tested (0.148 m s^{-1}) corresponds to the maximum flow rate in the lumen side (2500 ml min^{-1}) indicated in the brochure of the commercial hollow fiber contactor analyzed. Fig. 2(a) shows the effect on productivity and amine solution to carbon dioxide ratio. Productivity is estimated as

$$\alpha = \frac{F_{A,\text{in}}\theta N_{\text{fibers}}}{\pi R_{\text{shell}}^2 L_f} \tag{30}$$

and the lean carbon dioxide loading (LCL), and the amine solution to carbon dioxide ratio are calculated as

$$\text{LCL} = \frac{\text{total}[CO_2]_{\text{in}}}{\text{total}[\text{DEA}]} \tag{31}$$

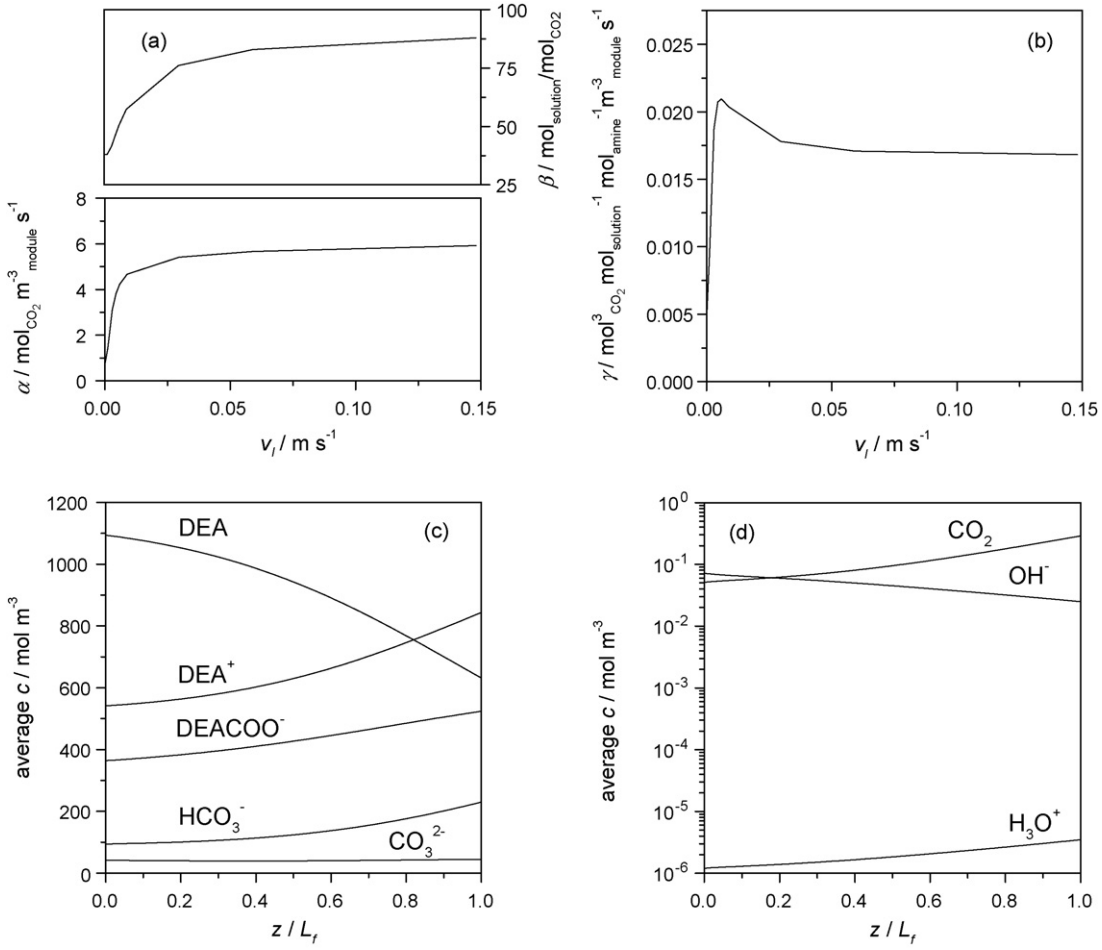

Fig. 2. Effect of liquid velocity on contactor performance. Total[DEA] = 2000 mol m^{-3}, total[H_2O] = 44,000 mol m^{-3}, LCL = 0.25. (a) Plots of α and β vs. v_l. (b) Plot of γ vs. v_l. (c and d) Profiles of $\bar{c}$ for the different species (except for H_2O, with a practically flat profile) along the hollow fibers for the optimum liquid velocity (5.9 × 10^{-3} m s^{-1}).

$$\beta = \frac{\text{total[DEA]} + \text{total[H}_2\text{O]}}{\bar{c}_{CO_2,out} + \bar{c}_{DEACOO,out} + \bar{c}_{HCO_3,out} + \bar{c}_{CO_3,out}} \quad (32)$$

It must be noted the total DEA and water concentration at the inlet and the outlet of the hollow fiber contactor are the same, because it is assumed that these components do not transfer to the gas phase. It is observed that reducing the liquid velocity leads to a decrease of amine solution to carbon dioxide ratio, especially at low velocities. This ratio tends to a minimum value, corresponding to equilibrium attainment. In this situation, the energy required for the amine regeneration per unit mass of carbon dioxide captured is minimum. However, it is also observed that the productivity diminishes when the liquid velocity decreases, which has already been verified experimentally elsewhere [30]. To minimize the volume of the membrane module required to treat a determined mole flow rate of carbon dioxide, it is necessary to work with the highest productivity possible, which is obtained with the highest liquid velocity. Hence, determining the values of the operational variables that result in the best performance among the ones studied in Fig. 2 is not an easy task, because the productivity and the amine solution to carbon dioxide ratio must be taken into account at the same time. Furthermore, the effect of the lean carbon dioxide loading on performance must also be considered, as it was commented before. This effect has not been considered previously in more comprehensive models proposed in the literature [30]. To simplify the comparison, assuming that the economic cost of the process is inversely proportional to productivity and LCL, and proportional to the amine solution to carbon dioxide ratio, the following parameter is proposed to evaluate the contactor performance, which must be as high as possible:

$$\gamma = \frac{\alpha \cdot \text{LCL}}{\beta} \quad (33)$$

The effect of liquid velocity on this parameter is depicted in Fig. 2(b). Now, an optimum performance is clearly observed with this variable. This result is different from the one found in other works [8,9], where it is proposed that high liquid velocities (above 0.1 m s^{-1}) are suitable for the operation of the contactor because they lead to higher carbon dioxide absorption fluxes. The difference comes from the inclusion of the effect of the amine solution to carbon dioxide ratio on performance.

The profiles of $\bar{c}$ for the different species along the hollow fibers for the optimum liquid velocity are given in Fig. 2(c) and (d). The conversion of free amine for the optimum velocity is about 42%, indicating that the best performance does not require very high amine depletion. It is also observed that the concentrations of bicarbonate and carbonate are lower than those of carbamate and protonated amine, but they are not negligible, leading to a significant difference between the concentration of carbamate and protonated amine. The concentrations of free carbon dioxide and hydroxide anions are quite low, which is consistent with the assumption that the reaction between carbon dioxide and hydroxyl anions does not contribute to the overall reaction rate in the CO_2–DEA–H_2O system [24].

Fig. 3 shows the effect of liquid velocity on contactor performance considering different assumptions in the kinetic model. The fixed conditions are: total [DEA] = 2000 mol m^{-3}, total[H_2O] = 44,000 mol m^{-3}, LCL = 0.4. The assumptions, grouped in four cases, are as follows:

- *Case I*. The deprotonation reactions are irreversible ($k_D^{-1} = 0$, $k_H^{-1} = 0$), other ions apart from carbamate, protonated amine and hydronium are not formed (reactions (6)–(8) do not take place), and the partition coefficient is constant, estimated in the absence of reaction between carbon dioxide and amine ($H = 0.5$ for the conditions analyzed in this work). This case is usually considered in the literature [5,7,9].
- *Case II*. The same as case I, but the deprotonation reactions are reversible (k_D^{-1} and k_H^{-1} are not zero).
- *Case III*. The same as case II, but bicarbonate and carbonate ions are formed (reactions (6)–(8) are at equilibrium).
- *Case IV*. The same as case III, but H depends on carbon dioxide loading as shown in Table 2.

It is observed that the effect of the reversibility of reactions (1)–(3) on productivity (and on the performance parameter) is quite strong, affecting the performance negatively, due to the reduction of the overall reaction rate. Therefore, it is deduced that the usual assumption of irreversible reactions can lead to overestimation of the performance for practical carbon dioxide loadings. When cases II and IV are compared, it is observed that the performance is similar. It must be noted that this similarity does not exists for lower carbon dioxide loadings (for LCL = 0.25, the maximum productivities for cases II and IV are 4.62 and 5.96 mol$_{CO_2}$ m^3 s^{-1}, respectively). The assumption of reversible reactions without the formation of carbonate and bicarbonate, implies that the maximum carbon dioxide loading is determined by the carbon dioxide–amine reaction stoichiometry. In this case, according to Boucif et al. [18], the stoichiometry is 1:2. This gives a maximum carbon dioxide loading of 0.5 mol/mol, which is unrealistic (carbon dioxide loadings in

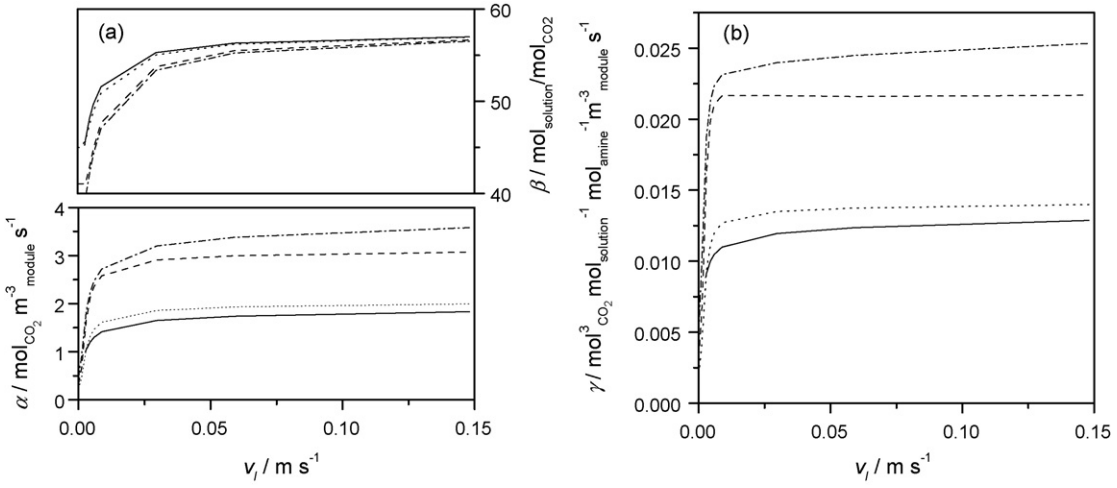

Fig. 3. Effect of liquid velocity on contactor performance for different model assumptions, grouped in four cases. The assumptions considered in each case are given in the text. (a) α and β. (b) Performance parameter defined in Eq. (33). Case I: dashed lines; case II: dotted lines; case III: dash-dotted lines; case IV: solid lines.

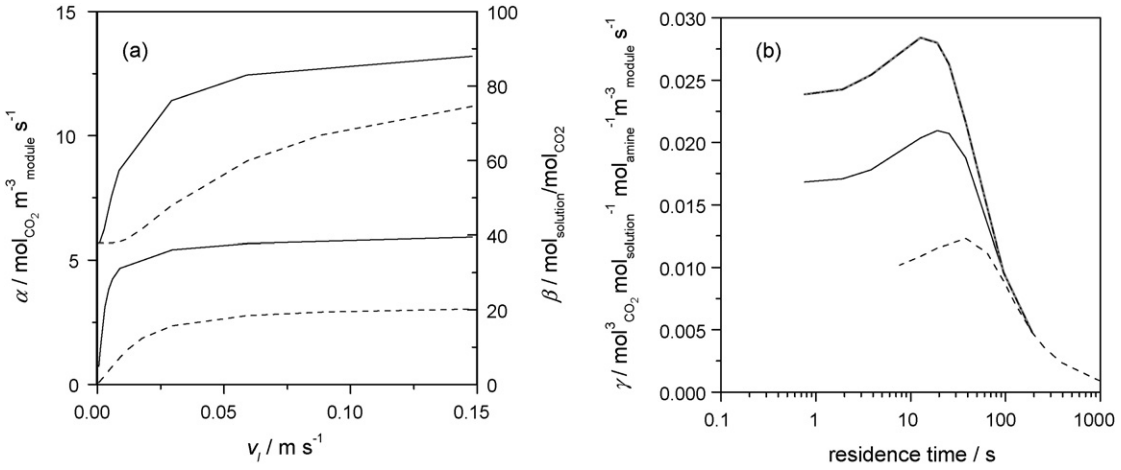

Fig. 4. Effect of fiber length on contactor performance. (a) Plots of α and β vs. v_l. (b) Plots of γ vs. residence time (L_f/v_l). Solid line, L_f = 0.113 m, dashed line, L_f = 1.13 m. The grey line corresponds to the case of $k_g = \infty$, L_f = 0.113 m, and the dashed-dotted line (overlapped) to the case of $k_g = \infty$, L_f = 1.13 m.

aqueous DEA of 1 mol/mol can be obtained in real systems [20]). Therefore, the employment of a kinetic model including the formation of these species is more advantageous, as a broader carbon dioxide loading range can be analyzed.

The effect of the formation of bicarbonate and carbonate (case III) is also quite strong, affecting the performance positively because the concentration of carbamate is reduced if these species are formed. This positive effect is compensated by the negative one of the reduction of H with carbon dioxide loading, if this reduction is taken into account (case III vs. case IV). The effect of carbon dioxide loading (or of amine concentration, discussed below) on the partition coefficient is not usually considered in the literature [8,30]. From this result, it is deduced that neglecting the variation of H may also result in overestimation of performance with realistic carbon dioxide loadings. Another important advantage of the kinetic model proposed in this work is that it opens the possibility of studying the carbon dioxide desorption from aqueous amine solutions in hollow fiber contactors, which is not possible with irreversible kinetic models.

3.2. Effect of fiber length

Fig. 4(a) shows the effect of increasing the fiber length on the plots of productivity and amine solution to carbon dioxide ratio vs. liquid velocity for the conditions of Fig. 2. It is observed that productivity decreases, in part because of the increase of module size with fiber length. It was checked that the mass transfer resistance on the shell side is not negligible, so that the increase of this resistance is also responsible for the decrease of productivity (as deduced from the effect of fiber length in Eq. (23)). On the other hand, the amine solution to carbon dioxide ratio decreases, because the increase of residence time (L_f/v_l) leads to a higher uptake of carbon dioxide per unit mass of amine solution. As the influence of fiber length is positive and negative at the same time, the overall effect on performance is not clear from these results. Fig. 4(b) shows the effect of increasing the fiber length on the plots of the performance parameter as a function of the residence time. The liquid velocity has been replaced by this variable to remove the effect of module size (only considering z-dimension) on the performance. The same plots in the case of absence of mass transfer resistance in shell side ($k_g = \infty$) are also included. It is observed that the contactor performance only depends on residence time in this case, regardless of the values of liquid velocity or fiber length. This is so because, if there is no resistance in the shell side, the independent variable z can be replaced by z/v_l in all of the differential equations of the proposed model, and the individual influence of fiber length and liquid velocity on productivity and amine solution to carbon dioxide ratio disappears. A negative effect of increasing fiber length on performance is now clear, due to the increase of resistance in the shell side.

3.3. Effect of lean carbon dioxide loading

The effect of the lean carbon dioxide loading on the maxima of the plots of performance parameter vs. v_l is shown in Fig. 5 (fixed conditions of case IV). For the highest lean carbon dioxide loading considered (LCL = 0.35), the maximum corresponds to the maximum liquid velocity. It is observed that there exists a value of lean carbon dioxide loading which yields an optimum value of the performance parameter (LCL = 0.3, $\alpha = 3.9\,\mathrm{mol_{CO_2}\,m^{-3}\,s^{-1}}$, $\beta = 51.55\,\mathrm{mol_{solution}/mol_{CO_2}}$). This optimum value appears because the lean carbon dioxide loading has two opposite effects: a direct positive effect, because the performance parameter is proportional to this variable (the regeneration energy decreases with LCL), and a negative effect due to reduction of free amine as LCL increases, which leads to a lower productivity.

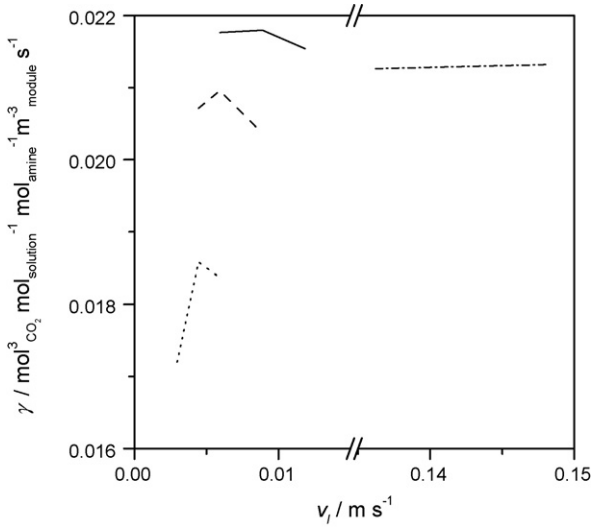

Fig. 5. Plots of γ vs. v_l for different lean carbon dioxide loadings. Dotted line, LCL = 0.2, dashed line, LCL = 0.25, solid line, LCL = 0.3, dash-dotted line, LCL = 0.35.

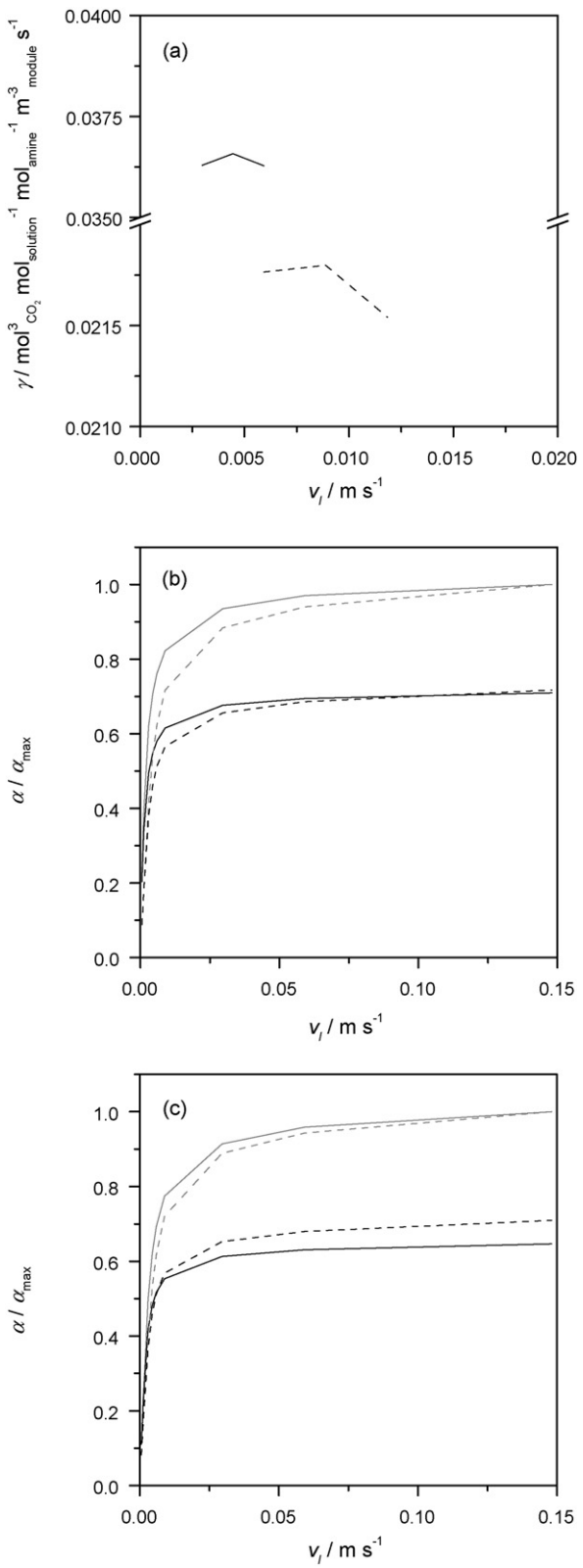

Fig. 6. (a) Plots of γ vs. v_l for different amine concentrations. Solid line, total[DEA] = 5000 mol m^{-3}, LCL = 0.2, dashed line, total[DEA] = 2000 mol m^{-3}, LCL = 0.3. (b) Plot of dimensionless productivity (see text) vs. v_l for total [DEA] = 2000 mol m^{-3} (dashed lines) and total [DEA] = 5000 mol m^{-3} (solid lines). Grey lines are obtained with $k_g = \infty$ and black lines with k_g estimated from Eq. (23). (c) The same plot as (b) with $H = 0.5$ for both amine concentrations.

3.4. Effect of amine concentration

Fig. 6(a) shows the effect of amine concentration (total [DEA] = 2 and 5 M) on the maxima of the plots of performance parameter vs. v_l. The water concentration for total [DEA] = 5 M is 28,000 mol m^{-3}. For the two concentrations analyzed, the maxima have been obtained with the optimum value of LCL (LCL = 0.3 for 2 M, and LCL = 0.2 for 5 M). The best value of the performance parameter with total [DEA] = 5 M is obtained with $\alpha = 3.99\,\text{mol}_{CO_2}\,\text{m}^{-3}\,\text{s}^{-1}$ and $\beta = 18.5\,\text{mol}_{solution}/\text{mol}_{CO_2}$. From these results, it is deduced that the optimum performance parameter improves when the amine concentration is increased within the range analyzed, mainly due to the reduction of the required amine solution to carbon dioxide ratio, whereas the productivity does not increase very much. The optimum value of the lean carbon dioxide loading decreases with amine concentration.

Amine concentration may also affect the shell mass transfer resistance because it has an influence on the carbon dioxide–amine reaction rate, and on the partition coefficient (Table 2), and thus it affects the carbon dioxide concentration gradient in the gas film in contact with the membrane. Fig. 6(b) shows the plots of productivity vs. v_l in the cases of absence and presence of shell side mass transfer resistance (k_g is infinite or is estimated with Eq. (23)) for amine concentrations of 2 and 5 M (LCL = 0.25). For each amine concentration, the two resulting curves are divided into the productivity obtained in the absence of shell side mass transfer resistance at the highest liquid velocity, α_{max} ($\alpha_{max} = 8.26$ and $4.89\,\text{mol}_{CO_2}\,\text{m}^{-3}_{module}\,\text{s}^{-1}$ for [DEA] = 2 and 5 M, respectively). In this plot, the difference between the curves at a given liquid velocity for the same amine concentration is indicative of the importance of shell side mass transfer resistance. It is observed that the effect of amine concentration on this resistance is small at high liquid velocities and it is more important (the resistance increases with amine concentration) at low liquid velocities (below 0.05 m s^{-1} approximately). The small effect at high liquid velocities is not expected, as the rate of reaction increases with amine concentration. This is attributed to the reduction of the partition coefficient with amine concentration (Table 2), which reduces the carbon dioxide concentration gradient in the gas film (Eqs. (19) and (20)). To check this hypothesis, the same comparison was carried out assuming the partition coefficient is constant ($H = 0.5$) for both amine concentrations (Fig. 6(c), $\alpha_{max} = 9.45$ and $12.76\,\text{mol}_{CO_2}\,\text{m}^{-3}_{module}\,\text{s}^{-1}$ for [DEA] = 2 and 5 M, respectively). Note the inversion of order of the maximum productivity when the variation of H with amine concentration is neglected, indicating that ignoring the effect of amine concentration on H has a strong impact on the simulated results. In this case, it is clearly observed that the shell side mass transfer resistance increases with amine concentration in all the range of liquid velocities.

4. Conclusions

The absorption of carbon dioxide from a carbon dioxide/nitrogen mixture into an aqueous DEA solution using a hollow fiber contactor has been simulated to obtain the effect of several operational variables (liquid velocity, fiber length, lean carbon dioxide loading, and amine concentration) on productivity and amine solution to carbon dioxide ratio. A kinetic model taking into account the effect of the reversibility of deprotonation steps and the distribution of products at equilibrium, including bicarbonate and carbonate anions, has been employed. These aspects should be taken into account for simulating this system because they affect the productivity and amine solution to carbon dioxide ratio rather strongly. A reduction of the liquid velocity leads to a decrease of amine solution to carbon dioxide ratio, tending to a minimum value, corresponding to

equilibrium attainment. At the same time, productivity decreases as liquid velocity is reduced. Assuming that the economic cost of the process is inversely proportional to productivity and lean carbon dioxide loading, and proportional to the amine solution to carbon dioxide ratio, a simple parameter is proposed to evaluate the contactor performance including these variables. There exists an optimum liquid velocity which maximizes this parameter if the rest of variables are constant. Increasing the fiber length has a negative effect on performance because of the increase of module size and the enhancement of the mass transfer resistance in the shell side. If mass transfer resistance in the shell side could be neglected, the contactor performance would depend on the residence time of the amine solution inside the fibers only, regardless of the individual values of fiber length and liquid velocity. There also exists an optimum value of the lean carbon dioxide loading, because increasing this parameter has a positive effect (reduction of the regeneration energy) and a negative effect (reduction of productivity) at the same time. The performance parameter improves when the amine concentration is increased within the range analyzed (total[DEA] = 2–5 M), mainly due to the reduction of the required amine solution to carbon dioxide ratio. Ignoring the effect of amine concentration on the partition coefficient has a strong impact on the simulated results. The effect of amine concentration on shell side mass transfer resistance at high velocities (above 0.05 m s^{-1} for the studied conditions) is small due to the combined effect of amine concentration on the carbon dioxide–amine reaction rate and the partition coefficient.

Nomenclature

$\bar{c}$	average concentration in the liquid phase (mol m^{-3})
c_A	carbon dioxide concentration in the liquid phase (mol m^{-3})
c_B	concentration of species different from molecular CO_2 in the liquid phase (mol m^{-3})
C_A	carbon dioxide concentration in the gas phase (mol m^{-3})
$C_{A,L}$	carbon dioxide concentration in the gas phase in contact with the liquid phase (mol m^{-3})
d_h	hydraulic diameter = 4 × free shell cross-sectional area/wetted perimeter (m)
$D_{A,g}$	effective diffusion coefficient of carbon dioxide in membrane pores (m^2 s^{-1})
$D_{A,m}$	molecular diffusivity of carbon dioxide in gas phase (m^2 s^{-1})
$D_{i,L}$	diffusivity of ith component in the liquid phase (m^2 s^{-1})
F_A	mole flow rate of carbon dioxide in the gas phase (mol s^{-1})
F_{N_2}	mole flow rate of carbon dioxide in the gas phase (mol s^{-1})
H	partition coefficient ($m^3_{gas}\ m^{-3}_{liquid}$)
k_D	kinetic constant defined in Eq. (2) (m^3 mol^{-1} s^{-1})
k_D^{-1}	kinetic constant defined in Eq. (2) (m^3 mol^{-1} s^{-1})
k_g	individual mass transfer coefficient in the shell side (m s^{-1})
k_H	kinetic constant defined in Eq. (3) (m^3 mol^{-1} s^{-1})
k_H^{-1}	kinetic constant defined in Eq. (3) (m^3 mol^{-1} s^{-1})
k_z	kinetic constant defined in Eq. (1) (m^3 mol^{-1} s^{-1})
k_z^{-1}	kinetic constant defined in Eq. (1) (s^{-1})
K	equilibrium constant (mol m^{-3})$^{(\text{moles of products} - \text{moles of reactants})}$
K_G	overall mass transfer coefficient between gas and liquid surface (m s^{-1})
l_m	membrane thickness (m)
L_f	fiber length (m)
LCL	lean carbon dioxide loading ($mol_{CO_2}\ mol^{-1}_{amine}$)
N_{fibers}	number of fibers
P	pressure (Pa)
r	radial coordinate (m)
r_i	reaction rate of ith component (mol m^{-3} s^{-1})
R	gas constant (J mol^{-1} K^{-1})
R_0	outer fiber diameter (m)
Re_g	Reynolds number ($d_h v_g \rho_g/\mu_g$)
R_{lm}	log-mean fiber radius (m)
R_{shell}	shell radius (m)
Sc_g	Schmidt number ($\mu_g/(\rho_g D_{A,m})$)
Sh_g	Sherwood number ($k_g d_h/D_{A,m}$)
T	temperature (K)
v_g	gas velocity = $(F_A + F_{N_2})RT/(P \times$ free shell cross-sectional area) (m s^{-1})
v_l	average liquid velocity (m s^{-1})
v_z	liquid velocity (m s^{-1})
x	dimensionless radial coordinate
z	axial coordinate (m)

Greek letters

α	productivity ($mol_{CO_2}\ m^{-3}_{module}\ s^{-1}$)
α_{max}	productivity at the highest liquid velocity in the absence of shell side mass transfer resistance ($mol_{CO_2}\ m^{-3}_{module}\ s^{-1}$)
β	amine solution to carbon dioxide ratio, defined in Eq. (32)
γ	performance parameter defined in Eq. (33)
ϕ	packing fraction = fiber volume/shell volume = $N_{fibers}(R_0/R_{shell})^2$
μ_g	gas viscosity (Pa s)
θ	fraction of carbon dioxide removal
ρ_g	gas density (kg m^{-3})

Subscripts

in	inlet
out	outlet
0	at $z = 0$

References

[1] U. Desideri, A. Paolucci, Performance modelling of a CO_2 removal system for power plants, Energy Conv. Manage. 40 (1999) 1899–1915.
[2] H. Herzog, What future for carbon capture and sequestration? Environ. Sci. Technol. 35 (2001) 148–153.
[3] IPCC, IPCC Special Report on Carbon Dioxide Capture and Storage, Cambridge University Press, United Nations, New York, 2005.
[4] K.A. Hoff, O. Juliussen, O. Falk-Pedersen, H.F. Svendsen, Modeling and experimental study of carbon dioxide absorption in aqueous alkanolamine solutions using a membrane contactor, Ind. Eng. Chem. Res. 43 (2004) 4908–4921.
[5] H.Y. Zhang, R. Wang, D.T. Liang, J.H. Tay, Modeling and experimental study of CO_2 absorption in a hollow fiber membrane contactor, J. Membr. Sci. 279 (2006) 301–310.
[6] H. Kreulen, C.A. Smolders, G.F. Versteeg, W.P.M. van Swaaij, Microporous hollow fiber membrane modules as gas–liquid contactors. Part 2. Mass transfer with chemical reaction, J. Membr. Sci. 78 (1993) 217–238.
[7] S.H. Yeon, B. Sea, Y.I. Park, K.H. Lee, Determination of mass transfer rates in PVDF and PTFE hollow fiber membranes for CO_2 absorption, Sep. Sci. Technol. 38 (2003) 271–293.
[8] R. Wang, D.F. Li, D.T. Liang, Modeling of CO_2 capture by three typical amine solutions in hollow fiber membrane contactors, Chem. Eng. Process. 43 (2004) 849–856.
[9] Y. Gong, Z. Wang, S. Wang, Experiments and simulation of CO_2 removal by mixed amines in a hollow fiber membrane module, Chem. Eng. Process. 45 (2006) 652–660.
[10] A. Malek, K. Li, W.K. Teo, Modeling of microporous membrane modules operated under partially wetted conditions, Ind. Eng. Chem. Res. 36 (1997) 784–793.
[11] A.M. Barbe, P.A. Hogan, R.A. Johnson, Surface morphology changes during initial usage of hydrophobic, microporous polypropylene membranes, J. Membr. Sci. 172 (2000) 149–156.
[12] J.L. Li, B.H. Chen, Review of CO_2 absorption using chemical solvents in hollow fiber membrane contactors, Sep. Purif. Technol. 41 (2005) 109–122.
[13] M. Mavroudi, S.P. Kaldis, G.P. Sakellaropoulos, A study of mass transfer resistance in membrane gas–liquid contacting processes, J. Membr. Sci. 272 (2006) 103–115.
[14] R. Wang, H.Y. Zhang, P.H.M. Feron, D.T. Liang, Influence of membrane wetting on CO_2 capture in microporous hollow fiber membrane contactors, Sep. Purif. Technol. 46 (2005) 33–40.

[15] V.Y. Dindore, D.W.F. Brilman, P.H.M. Feron, G.F. Versteeg, CO_2 absorption at elevated pressures using a hollow fiber membrane contactor, J. Membr. Sci. 235 (2004) 99–109.
[16] A.N.M. Peeters, A.P.C. Faaij, W.C. Turkenburg, Techno-economic analysis of natural gas combined cycles with post-combustion CO_2 absorption, including a detailed evaluation of the development potential, Int. J. Greenhouse Gas Control I (2007) 396–417.
[17] R. Sakwattanapong, A. Aroonwilas, A. Veawab, Behavior of reboiler heat duty for CO_2 capture plants using regenerable single and blended alkanolamines, Ind. Eng. Chem. Res. 44 (2005) 4465–4473.
[18] N. Boucif, E. Favre, D. Roizard, CO_2 capture in HFMM contactor with typical amine solutions: a numerical analysis, Chem. Eng. Sci. 63 (2008) 5375–5385.
[19] S. Paul, A.K. Ghoshal, B. Mandal, Theoretical studies on separation of CO_2 by single and blended aqueous alkanolamine solvents in flat sheet membrane contactor (FSMC), Chem. Eng. J. 144 (2008) 352–360.
[20] M. Mofarahi, Y. Khojasteh, H. Khaledi, A. Farahnak, Design of CO_2 absorption plant for recovery of CO_2 from flue gases of gas turbine, Energy 33 (2008) 1311–1319.
[21] P.V. Danckwerts, The reaction of CO_2 with alkanolamines, Chem. Eng. Sci. 34 (1979) 443–446.
[22] R.J. Littel, G.F. Versteeg, W.P.M. Swaaij, Kinetics of CO_2 with primary and secondary amines in aqueous solutions. II. Influence of temperature on zwitterions formation and deprotonation rates, Chem. Eng. Sci. 47 (1992) 2037–2045.
[23] G.F. Versteeg, W.P.M. van Swaaij, On the kinetics between CO_2 and alkanolamines both in aqueous and non-aqueous solutions. I. Primary and secondary amines, Chem. Eng. Sci. 43 (1988) 573–587.
[24] S.H. Ali, Kinetic study of the reaction of diethanolamine with carbon dioxide in aqueous and mixed solvent systems—application to acid gas cleaning, Sep. Purif. Technol. 38 (2004) 281–296.
[25] S. Lee, S. Maken, J.W. Park, H.J. Song, J.J. Park, J.G. Shim, J.H. Kim, H.M. Eum, A study on the carbon dioxide recovery from 2 ton-CO_2/day pilot plant at LNG based power plant, Fuel 87 (2008) 1734–1739.
[26] P.H.M. Feron, A.E. Jansen, CO_2 separation with polyolefin membrane contactors and dedicated absorption liquids: performances and prospects, Sep. Purif. Technol. 27 (2002) 231–242.
[27] R. Prasad, K.K. Sirkar, Dispersion-free solvent extraction with microporous hollow-fiber modules, AIChE J. 34 (1988) 177–188.
[28] R.B. Bird, W.E. Stewart, E.N. Lightfoot, Transport Phenomena, Wiley, New York, 1960.
[29] D.O. Cooney, S.S. Kim, E.J. Davis, Analysis of mass transfer in hemodialysers for laminar blood flow and homogeneous dialysate, Chem. Eng. Sci. 29 (1974) 1731–1738.
[30] M. Al-Marzouqi, M.H. El-Naas, S. Marzouk, N. Abdullatif, Modeling of chemical absorption of CO_2 in membrane contactors, Sep. Purif. Technol. 62 (2008) 499–506.